MPP-2008-15
UB-ECM-PF-08/06

FCNC-induced heavy-quark events at the LHC from Supersymmetry

Santi Béjar[a], **Jaume Guasch**[b,d], **David López-Val**[c,d], **Joan Solà**[c,d]

[a] Max-Planck-Institut für Physik,
Föhringer Ring 6, D–80805 München, Germany
[b] Gravitation and Cosmology Group, Dept. FF, Univ. de Barcelona
Av. Diagonal 647, E-08028 Barcelona, Catalonia, Spain
[c] High Energy Physics Group, Dept. ECM, Univ. de Barcelona
Av. Diagonal 647, E-08028 Barcelona, Catalonia, Spain
[d] Institut de Ciències del Cosmos, UB, Barcelona.
E-mails: sbejar@mppmu.mpg.de, jaume.guasch@ub.edu, dlopez@ecm.ub.es, sola@ifae.es.

Abstract

We analyze the production and subsequent decay of the neutral Higgs bosons $h \equiv \mathrm{h}^0, \mathrm{H}^0, \mathrm{A}^0$ of the MSSM into electrically neutral quark pairs of different flavors ($qq' \equiv tc,\ bs$, depending on h) at the LHC, i.e. $\sigma(\mathrm{pp} \to h \to qq')$, and compare with the direct FCNC production mechanisms $\sigma(\mathrm{pp} \to qq')$. The cross-sections are computed in the unconstrained MSSM with minimal flavor-mixing sources and taking into account the stringent bounds from $\mathrm{b} \to \mathrm{s}\gamma$. We extend the results previously found for these FCNC processes, which are singularly uncommon in the SM. Specifically, we report here on the SUSY-EW part of $\sigma(\mathrm{pp} \to h \to qq')$ and the SUSY-QCD and SUSY-EW contributions to $\sigma(\mathrm{pp} \to bs)$. In this way, the complete map of MSSM predictions for the qq'-pairs produced at the LHC becomes available. The upshot is that the most favorable channels are: 1) the Higgs boson FCNC decays into bs, and 2) the direct production of tc pairs, both of them at the $\sim$ 1pb level and mediated by SUSY-QCD effects. If, however, the SUSY-QCD part is suppressed, we find a small SUSY-EW yield for $\sigma(\mathrm{pp} \to h \to tc)_{\max} \sim 10^{-4}$pb but, at the same time, $\sigma(\mathrm{pp} \to h \to bs)_{\max} \sim 0.1 - 1\,\mathrm{pb}$, which implies a significant number ($\sim 10^4 - 10^5$) of bs pairs per $100\,\mathrm{fb}^{-1}$ of integrated luminosity.

1 Introduction

The upcoming generation of TeV-class colliders, headed by the imminent startup of the Large Hadron Collider (LHC) at CERN, will offer us the opportunity to dig deeper than ever into the nature of fundamental interactions. Despite its successful career, the Standard Model (SM) of elementary particles still offers a number of intriguing puzzles to be resolved, such as the ultimate origin of the electroweak (EW) symmetry breaking and the mass generation mechanism. Among the wide set of theoretical proposals that have been conjectured so far, the possibility that the fundamental laws of Nature exhibit a symmetry between fermionic and bosonic degrees of freedom – that is, supersymmetry (SUSY) and most particularly the Minimal Supersymmetric Standard Model (MSSM) [1] – has been postulated as one of the firmest candidates to account for possible scenarios of physics beyond the SM, i.e. of New Physics (NP).

The quest for experimental signatures of an underlying SUSY dynamics is undoubtedly one of the major endeavors for the LHC. Besides the direct production and tagging of SUSY particles

(which could be cumbersome in practice), it is of great interest to consider the impact of SUSY radiative corrections on conventional processes in the SM. In such cases the enhancement capabilities associated to the non-standard couplings may provide sources of genuine NP signatures. This possibility was thoroughly analyzed in the past for the W and Z boson physics (see e.g. [2, 3]).

More recently, a great deal of attention has been devoted to processes triggered by Flavor-Changing Neutral-Current (FCNC) sources beyond the SM, in particular from SUSY interactions. From the seminal work of Glashow, Iliopoulos and Maiani (GIM) [4] it has been known that the FCNC interactions are absent at the tree level within the SM and, most significantly, they are largely suppressed at the 1-loop order. This, so-called, GIM mechanism is an in-built feature of the mathematical core of the SM, thanks to the unitarity of the CKM matrix. Low energy B-meson physics, for example, provides a number of well-measured FCNC processes, such as the B-meson radiative decay $\mathrm{b} \to \mathrm{s}\gamma$. Its branching ratio reads $B(\mathrm{b} \to \mathrm{s}\gamma) = (2.1 - 4.5) \times 10^{-4}$ at the 3σ level [5]. This important and well studied process can be used to constrain models of NP that predict non-standard flavor-changing interactions. In contrast, the FCNC effects involving the top quark as an external particle turn out to be dramatically suppressed by the GIM mechanism. The predicted branching ratios are at the level of $B(\mathrm{t} \to \mathrm{cg}) \sim 10^{-11}$ and $B(\mathrm{t} \to \mathrm{c}H) \sim 10^{-14}$ [6], hence far below the limits of observability.

In stark contrast with this meager SM panorama, the MSSM opens new vistas for a fruitful FCNC physics of the top quark. A most remarkable example is the case of the top quark decay into the lightest supersymmetric neutral Higgs boson, h^0, whose branching ratio could be of order $B(\mathrm{t} \to \mathrm{ch}^0) \sim 10^{-4} - 10^{-3}$ [7] – previously underestimated in [8]. A branching ratio of this order represents not only an enhancement of 10 orders of magnitude above the SM prediction, but it opens the realistic possibility for measurement. The origin of these possible effects lies in the richer diversity of sources of flavor mixing in the MSSM, in particular among fermion and sfermions of the same charge and different generation. They ultimately stem from the so-called misalignment of the squark mass matrices with respect to the quark ones and can be described by means of the parameters δ_{ij}^{AB} (being $A, B = L, R$ the chirality indices and $i, j = 1, 2, 3$ the flavor ones). A generic entry of the soft SUSY-breaking squark mass matrix reads $(M^2)_{ij}^{AB} = \delta_{ij}^{AB}\, \tilde{m}_i\, \tilde{m}_j$ (for $i \neq j$). As a consequence, new types of FCNC couplings arise and they need not be subdued by GIM suppression. Obviously, such scenarios bring us some hope to effectively unearth hints of SUSY physics out of the study of both low energy and high energy FCNC processes [9].

Interestingly enough, not only SUSY can help here; other alternative proposals of extended physics beyond the SM, among them the general Two-Higgs-Doublet Models (2HDM) [10], top-color models and strong flavor-changing effects predict in some cases an enhanced, and sometimes distinctive, FCNC phenomenology [11–14]. Attentive studies on this field can thus be of great help in seeking for new signatures and eventually disentangling the sort of NP hiding right there.[1]

In this letter, we wish to further elaborate on the rich phenomenology of flavor-changing processes in the MSSM, specifically on those that could lead to an unsuspected overproduction rate of electrically-neutral heavy-quark pairs qq' of different flavors at the LHC. Most conspicuously, we have the process of single top quark production induced by FCNC, i.e. any of the two-body final states $\mathrm{pp} \to tc \equiv \mathrm{t}\overline{\mathrm{c}} + \overline{\mathrm{t}}\mathrm{c}$. This process is extremely suppressed in the SM, while it can be highly enhanced in the MSSM [16–20]. A similar situation applies to producing FCNC single b-events, i.e. $bs \equiv \mathrm{b}\overline{\mathrm{s}} + \mathrm{s}\overline{\mathrm{b}}$, although here the SM suppression is not so drastic as in the tc case.

There are different supersymmetric mechanisms leading to enhanced tc and bs final states. As a first possibility, we have the SUSY flavor-changing charged (and neutral) currents contributing to the direct production processes $\mathrm{pp} \to tc$ and $\mathrm{pp} \to bs$. An alternative mechanism to produce these final states is through the production and subsequent FCNC decay of a neutral Higgs boson, i.e.

[1] For a review of top quark and Higgs boson FCNC physics in the MSSM and in general 2HDM models, see e.g. [15] and references therein.

$pp \to h \to tc$ and $pp \to h \to bs$. This mechanism was explored within the context of the general 2HDM [12], in which $h = h^0, H^0, A^0$ [10], and it was later revisited within the unconstrained MSSM through the strong supersymmetric (SUSY-QCD) corrections to the Higgs boson FCNC branching ratios into the heavy-quark final states [21, 22]. However, a first computation of the corresponding LHC production rates appeared only in [23].

Supersymmetric electroweak (SUSY-EW) contributions to neutral Higgs boson decays could be important too. These effects can be induced, in principle, by both charged and neutral currents. The latter are triggered by the neutralinos and some authors have dealt with these effects [24–26]. Here, however, following [7] (see also [27]), we compute the SUSY-EW contributions in the super-CKM basis, i.e. under the assumption of minimal flavor violation ($\delta_{ij}^{AB} = 0,\ i \neq j$). We argue and verify that the neutralino effects are subleading. Therefore, we concentrate on the charged current sector of the electroweak MSSM Lagrangian [28]. In this setup, we perform a systematic analysis along the lines of [23] by addressing the SUSY-EW effects on $\sigma(pp \to h \to qq')$ induced by charginos, squarks and charged Higgs bosons in the MSSM. We also compute the pay-off in the number of bs events from the direct production mechanism $\sigma(pp \to bs)$ within the MSSM, including both SUSY-QCD and SUSY-EW effects. Notice that the interest of knowing the SUSY-EW effects in these studies is that they could be the only sizeable supersymmetric source of FCNC qq'-pairs at the LHC, if gluinos turn out to be very heavy and/or the inter-generational mixing parameters would be too small or simply zero [2].

2 Higgs boson decays into neutral heavy quark-pairs

In this section, we discuss the general expectations on the production cross-section of electrically neutral pairs of heavy quarks of different flavors at the LHC, whose origin stems from the FCNC decays of a neutral MSSM Higgs boson [10]. The main contribution to the overall process may be sequentially split into: i) production of a real neutral Higgs boson in a proton-proton collision, ii) followed by its decay through loop diagrams contributing to the FCNC final state. Assuming that the Higgs bosons are produced on-shell, the total production rate can be factorized as follows:

$$\begin{aligned} \sigma(pp \to h \to qq') &\equiv \sigma(pp \to hX) B(h \to qq') \\ &\equiv \sigma(pp \to hX) \frac{\Gamma(h \to qq')}{\Gamma(h \to Y)} \quad (qq' \equiv bs \text{ or } tc)\,. \end{aligned} \tag{1}$$

Here $\Gamma(h \to qq')$ is the total FCNC two-body partial decay width of the corresponding MSSM Higgs boson $h = h^0, H^0, A^0$ into the (kinematically possible) neutral states $bs \equiv b\overline{s} + s\overline{b}$ or $tc \equiv t\overline{c} + \overline{t}c$; and $\Gamma(h \to Y)$ stands for the – consistently computed – total decay width in each case.

Before coming to grips with the full numerical analysis, it is always a good exercise to perform an analytical estimate based on physical considerations. In doing this, we expect to gain insight into the dominant FCNC sources of enhancement within the MSSM and roughly predict (within order of magnitude, hopefully) the relation between the cross-sections $\sigma(pp \to h \to tc)$ and $\sigma(pp \to h \to bs)$. In order to address such estimate, we first need to specify the possible supersymmetric electroweak contributions to the FCNC Higgs boson decays into the heavy-quark final states under consideration. For the sake of definiteness, let us concentrate on H^0 (i.e. the heavy CP-even Higgs boson of the MSSM). A sample of Feynman diagrams from the SUSY-EW sector is displayed in Fig. 1. The overall set is, of course, UV finite (as we have checked). However, we note that the subsets of charged gauge and Higgs boson mediated diagrams, on the one hand, and the

[2] When considering the explicit FCNC effects on our processes, we just focus on $\delta_{23} \equiv \delta_{23}^{LL}$. We assume that the FCNC mixing may hold in the chiral LL sector of the squark 6×6 mass matrices only, which is well motivated theoretically. The other chirality sectors give similar contributions [7]. See also [16, 18].

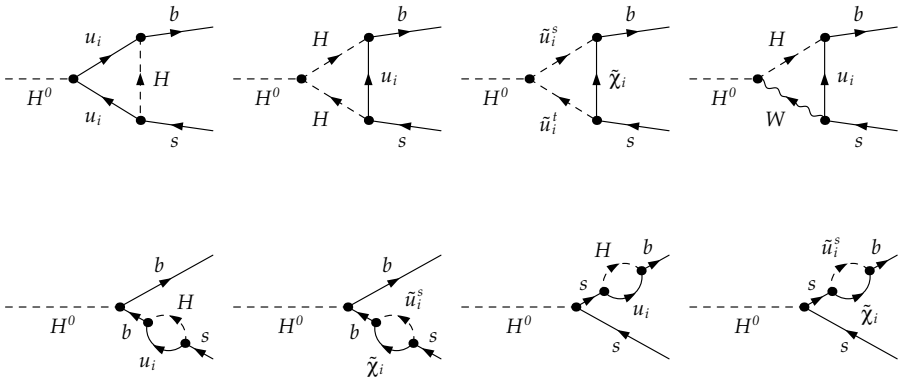

Figure 1: Sample of SUSY-EW contributions to the decay of the Higgs boson H^0 into bs from the charged current. The electroweak effects that could originate from the neutralinos are not shown. A similar collection of diagrams describes the corresponding decay into tc.

chargino mediated, on the other, are separately UV-finite. Moreover, each of these subsets involves two different topologies, vertex corrections (V) and wave-function (WF) renormalization, whose respective contributions are also separately UV-finite after summation over generations.

It turns out that the chargino-mediated pieces drive the bulk of the contribution, basically because they are not suppressed by the GIM mechanism. Let us first consider the WF corrections. Using no other tools than dimensional analysis, power counting, CKM matrix elements and dynamical features, we can estimate the (one-loop) decay width of $H^0 \to bs$ as follows:

$$\Gamma_{bs}^{\rm WF} \;\sim\; m_H\, G_F^3 \left(\frac{m_t^2\, m_b}{M_{SUSY}^2}\right)^2 \left(\frac{V_{ts}\, V_{tb}^*}{16\pi^2}\right)^2 \left(A_t - \frac{\mu}{\tan\beta}\right)^2 \left(\frac{\mu\, \cos\alpha}{\cos^2\beta\, \sin\beta}\right)^2 , \qquad (2)$$

and similarly for the $H^0 \to tc$ channel:

$$\Gamma_{tc}^{\rm WF} \;\sim\; m_H\, G_F^3 \left(\frac{m_t\, m_b^2}{M_{SUSY}^2}\right)^2 \left(\frac{V_{tb}\, V_{bc}^*}{16\pi^2}\right)^2 (A_b - \mu\tan\beta)^2 \left(\frac{\mu\, \sin\alpha}{\cos\beta\, \sin^2\beta}\right)^2 . \qquad (3)$$

Let us briefly explain the origin of the different terms appearing in the expressions above. In both cases we include the standard numerical factor arising from the loop integration. G_F stands for the Fermi constant, and $V_{tb} \sim 1, V_{bc} \sim 0.02, V_{ts} \sim 0.02$ are the CKM matrix elements; M_{SUSY} defines a common scale for the soft SUSY-breaking masses (of squarks and gauginos), the MSSM trilinear couplings are labelled by A_b, A_t; and μ indicates the higgsino mass parameter. The latter accounts for the helicity flip that appears along the chargino line[3]. The angle α is the mixing angle between the neutral CP-even Higgs boson states. Finally, $\tan\beta \equiv v_2/v_1$ is the ratio of vacuum expectation values of the two MSSM Higgs doublets [10]. A key element in the expressions above is the factor associated to the chiral transition of top squarks, $m_t\,(A_t - \mu\tan\beta)$, or bottom squarks, $m_b\,(A_b - \mu\tan\beta)$, depending on the case. In the estimate, we also include the Higgs-quark-quark and (the leading part of) the chargino-quark-squark couplings [10], from which we get the remaining dependences in α, β. Last but not least, we also keep track of the relevant mass scales arising from the 2-point loop functions and the phase space integration, which we settle in terms of M_{SUSY} and the mass of the decaying Higgs particle, m_H. Note that equation (2), for example, patently reveals different sources of possible large enhancements, mainly associated with large values of

[3]For an explanation and a computation of the helicity flips in the quark propagator, see e.g. Refs. [29], specifically Fig. 7 and eq. (76) of the first work in [29].

the trilinear coupling A_t, the higgsino mass parameter μ and/or the trigonometric factor $1/\cos^4\beta$ (which behaves as $\sim \tan^4\beta$ in the large $\tan\beta$ regime).

Similar arguments can be applied to the vertex corrections, and we arrive at

$$\Gamma^{\rm V}_{bs} \;\sim\; m_H\, G_F^3 \left(\frac{V^*_{tb}\, V_{ts}}{16\pi^2}\right)^2 \left(\frac{m_t^2\, m_b}{M^2_{SUSY}}\right)^2 \left[\frac{\mu\,(A_t \sin\alpha - \mu\cos\alpha)}{\sin^2\beta\,\cos\beta}\right]^2 , \tag{4}$$

$$\Gamma^{\rm V}_{tc} \;\sim\; m_H\, G_F^3 \left(\frac{V_{tb}\, V^*_{bc}}{16\pi^2}\right)^2 \left(\frac{m_t\, m_b^2}{M^2_{SUSY}}\right)^2 \left[\frac{\mu\,(A_b \cos\alpha - \mu\sin\alpha)}{\sin\beta\,\cos^2\beta}\right]^2 . \tag{5}$$

Some differences between the formulae above corresponding to tc and bs final states are worth noticing. For instance, the quark (or squark) mass insertions involve distinct mass factors: m_b (in the tc case) and m_t (in the bs one). The trigonometric couplings are also different and for this reason one of the channels may be much more suppressed than the other at different regimes. In particular, we see that in both cases the decay rate increases with $\tan\beta$, but while the leading effect of the bs channel lies in the WF corrections the dominant one in the tc channel resides in the V contribution. As for the neutralino yield (whose diagrammatic effects are not shown in Fig. 1), similar analytical estimates can be produced. We limit ourselves to single out some differences. To start with, we emphasize that these contributions are proportional to the inter-generational mixing parameters and are, therefore, vanishing for $\delta^{AB}_{ij} = 0\,(i \neq j)$. The corresponding effects in the WF sector are such that e.g. the factors $A_b - \mu\tan\beta$ and $A_t - \mu/\tan\beta$ become interchanged in the counterparts of Eqs. (2)-(3). Similarly with the factors $A_t\sin\alpha - \mu\cos\alpha$ and $A_b\cos\alpha - \mu\sin\alpha$ in the corresponding vertex contributions, i.e., the analogous of Eqs. (4)-(5).

In sections 4-5, we will come back to the previous analytical estimates and shall compare them with the exact numerical results. This will be useful to track the dynamical origin of the leading MSSM contributions and, in particular, to argue that the neutralino effects are negligible.

Similar considerations can be done for the other Higgs bosons. However, we recall that $\rm h^0$ (the lightest CP-even Higgs boson) cannot decay into tc because $m_{\rm h^0} < m_t$ in the MSSM. Moreover, for this Higgs boson, the implications of the so-called "small α_{eff}" scenario (triggered by large radiative corrections in the parameters of the MSSM Higgs sector) must be taken into account [30].

3 Framework for the numerical analysis

In order to compute the SUSY-EW one-loop diagrams contributing to the FCNC cross-sections $\sigma(\rm pp \to h \to qq')$ for the three MSSM neutral Higgs bosons ($h = \rm h^0, H^0, A^0$), we shall closely follow the notation and methods of Refs. [7, 11, 12, 22, 23]. We address the reader to these references for the technical details. In particular, a thorough exposition of the relevant interaction Lagrangians and similar set of Feynman diagrams for the FCNC interactions, is provided in [7]. See also Ref. [10] for basic definitions in the MSSM framework and [29] for detailed computational techniques and further illustration of the supersymmetric enhancement effects in other relevant Higgs boson processes. Along our computation we have made use of `HIGLU`, `PPHTT` [31], `LoopTools`, `FeynArts` and `FormCalc` [32].

For the numerical evaluation, we shall adhere (wherever possible) to the general procedure put forward in Ref. [23], where significant parts of the numerical contributions to the cross-sections have already been reported. Next we specify the framework under which the computation of the observables (1) has been carried out in the present work:

- We compute the one-loop SUSY-EW contributions to the FCNC partial decay widths $\Gamma(h \to qq')$ and compare with the corresponding SUSY-QCD effects [23];

- The SUSY-EW part is defined to be the set of contributions from charginos, neutralinos and Higgs bosons. In practice, however, we will provide the detailed results from the charged current effects, and argue (and numerically verify) that the neutralino contributions are comparatively negligible.

Our major goal is to assess what are the theoretical expectations on the observables (1) within the MSSM and, most particularly for the present work, to ascertain whether in the absence of strong supersymmetric sources of FCNC the electroweak SUSY sector can still provide significant rates. To this aim we have performed a systematic scan all over the MSSM parameter space and have determined the maximum values for the production rates (1) under study. Furthermore, in order to keep the CPU-time under a feasible range, such a scan has been carried out by means of a Monte Carlo sampling method [33] based on the well-known Vegas integration program [34]. This numerical procedure was amply tested in the similar computation presented in Ref. [23].

On this basis, we have performed a maximization of the FCNC cross-section within the following restrictions:

$\tan\beta$	50
A_t	$\lvert A_t\rvert \leq 3M_{\rm SUSY}$
A_b	$\lvert A_b\rvert \leq 3M_{\rm SUSY}$
μ	$(0\cdots 1000)\,{\rm GeV}$
$m_{\tilde{q}_i}$	$m_{\tilde{d}_{\rm L}} = m_{\tilde{d}_{\rm R}} = m_{\tilde{u}_{\rm R}} = m_{\tilde{g}} \equiv M_{\rm SUSY}$
M_2	$M_{\rm SUSY}$
$M_{\rm SUSY}$	$(150\cdots 1000)\,{\rm GeV}$
m_{A^0}	$(100\cdots 1000)\,{\rm GeV}$
$M_{\tilde{q}_i}$	$2\,M_{\tilde{q}_i} > m_{H^0} + 50\,{\rm GeV}$
	$M_{\tilde{q}_i} + M_{\tilde{q}_j} > m_{A^0} + 50\,{\rm GeV}$ $(i \neq j)$
$B({\rm b}\to{\rm s}\gamma)$	$(2.1 - 4.5)\times 10^{-4}$ $\quad(3\sigma)$

(6)

Here $m_{\tilde{q}_i} = m_{\tilde{q}_{L,R}}$ are the squark soft SUSY-breaking mass parameters in each chiral sector, which are common for the three generations; $M_{\tilde{q}_i}$ are the physical masses of the squarks, M_2 is the $SU(2)_L$ gaugino mass, and m_h stands for the mass of the corresponding Higgs boson $h = {\rm h}^0, {\rm H}^0, {\rm A}^0$. Due to the structure of the couplings in the MSSM, and taking into account that the range $\tan\beta \lesssim 2.5$ is not favored in the MSSM, the parameter $\tan\beta$ is fixed at a high value for both channels as indicated. Concerning the characteristic SUSY mass parameter $M_{\rm SUSY}$, it sets the scale for the masses of the squarks and gauginos. Notice also that our analysis incorporates a specific choice of sign for μ (> 0) partially motivated by the data on the muon anomalous magnetic moment [4]. We adopt $B({\rm b}\to{\rm s}\gamma) = (2.1 - 4.5)\times 10^{-4}$ as the experimentally allowed range at the 3σ level [5] and include in our codes the MSSM computation of the branching ratio at leading order from Ref. [36]. In addition, we make sure that the sign of the MSSM amplitude for ${\rm b}\to{\rm s}\gamma$ and the purely-SM one do coincide [37]. By enforcing these experimental and theoretical constraints in our calculation, we automatically eschew regions of the MSSM parameter space which would artificial enhance the predicted qq' rates at the LHC.

Concerning the numerical computation of the direct bs production ${\rm pp}\to bs$ (mainly from gluon-gluon fusion ${\rm pp(gg)}\to bs$), some technical stumbling blocks have to be overcome. On the one hand, it is well-known that the presence of light quarks in the final state of such type of processes entails large logarithmic factors, which depend on the soft scales of the problem – precisely the masses of these light quarks. These large logarithms are the remnants of the truly collinear divergences that would arise if quarks were massless, and they turn out to be related to the non-perturbative

[4] The sign $\mu > 0$ is not essential for our numerical results. Moreover, the observable $g_\mu - 2$ also depends on the value of some slepton masses which do not play any role in our calculation. For the SUSY effects on $g_\mu - 2$, see e.g. the excellent review [35] and references therein.

regime of QCD. Upon resummation, these terms can be factored out from the computation of the partonic cross section, and finally reabsorbed into the definition of the parton fragmentation functions. Nevertheless, we do not need to address such a detailed analysis here. Instead, we can include an angular cut ($\sin^2\theta \geq 0.05$) to circumvent such delicate collinear scenario. Such a simpler strategy should be enough to attest the fact that the direct production of bs is, by far, a subleading mechanism – See Section 4 for details.

A second (and even more subtle) difficulty is caused because the bs production threshold is very small. In the limit of very low external momenta (which is, by the way, the situation when we probe partonic $\sqrt{S}$ energies near the bs threshold), we encounter one-loop expressions of the sort

$$\mathcal{M} \sim \int d^4 q \, \frac{f(q)}{((q+\epsilon)^2 - m_1^2)\ (q^2 - m_1^2)} \cdots \tag{7}$$

where $\epsilon \ll m_1$. This kind of expression, when evaluated numerically, generates pseudo-singularities of the kind $\mathcal{O}(1/\epsilon^2)$ in some of the intermediate steps, a fact that is reflected in the associated integration uncertainties. Numerical instabilities have a critical impact on the overall computation, which involves a large number of diagrams (some of them including various "box diagrams", i.e. 4-point functions). We refrain from displaying here the full list of diagrams, which is very similar to those shown in Figs. 1-5 of Ref. [20], after appropriately replacing the virtual quark and squark contributions in accordance with the new external b and s states. Particularly subtle are the instabilities involved in solving the Passarino-Veltman reduction formulae necessary to obtain the 4-point amplitudes (a cumbersome diagonalization procedure which is extremely sensitive to numerical niceties).

A thorough analysis of such instabilities has been performed, from which we conclude that we can handle them by: i) changing the subroutine that undertakes the Passarino-Veltman reduction for the 4-point amplitudes within the LoopTools framework – we use, instead, an independent version presented in [38], which is also implemented in the LoopTools code but only used to cross-check the results in the standard setup. This way the problem is smoothed, albeit not fully solved since the new subroutine renders lower uncertainties in such delicate regimes; and ii) introducing a cut over the partonic integration domain in order to elude the neighboring region of the bs threshold where the numerical instabilities arise.

4 Numerical analysis of the bs production rate

Let us first consider the Higgs boson production/decay mechanism $pp \to h \to bs$. The main result of our Monte Carlo scan is shown in Fig. 2a, which displays the maximum values of the production cross-section $\sigma(pp \to h \to bs)$, Eq. (1), for the three MSSM Higgs bosons $h = h^0, H^0, A^0$ at the LHC as a function of m_{A^0}. On the left-vertical axis of this figure, we indicate the value of the cross-section (in pb) and at the same time we track the number of FCNC events (per 100 fb^{-1} of integrated luminosity $\int \mathcal{L}\, dt$) on the right vertical axis. One can immediately see that, in the large $\tan\beta$ regime: i) The maximum number of events reaches a sizeable level, which lies between 10^4 and 10^5 per $\int \mathcal{L}\, dt = 100$ fb^{-1} in the interesting mass region $100\,\text{GeV} \lesssim m_{A^0} \lesssim 200\,\text{GeV}$. In the particular case of the h^0 channel, the rate of $\sim 10^4$ events extends even farther for larger m_{A^0} (up to around 250 GeV); ii) Actually, for this channel, there is an approximate plateau extending across the mass range $300\,\text{GeV} \lesssim m_{A^0} \lesssim 600\,\text{GeV}$, where the event rate $\sim 10^3$ is sustained; iii) The other two channels H^0, A^0 can reach a similar (though smaller) maximum number of events, but only in the strict range $100\,\text{GeV} \lesssim m_{A^0} \lesssim 200\,\text{GeV}$ beyond which the rate decreases steadily and unstoppably. We can compare this behavior with the SUSY-QCD case [23] – see Fig. 2b – which looks similar but significantly shifted upwards. For a better understanding of these results, in Fig. 3a we show the corresponding FCNC decay branching ratio for the MSSM parameters

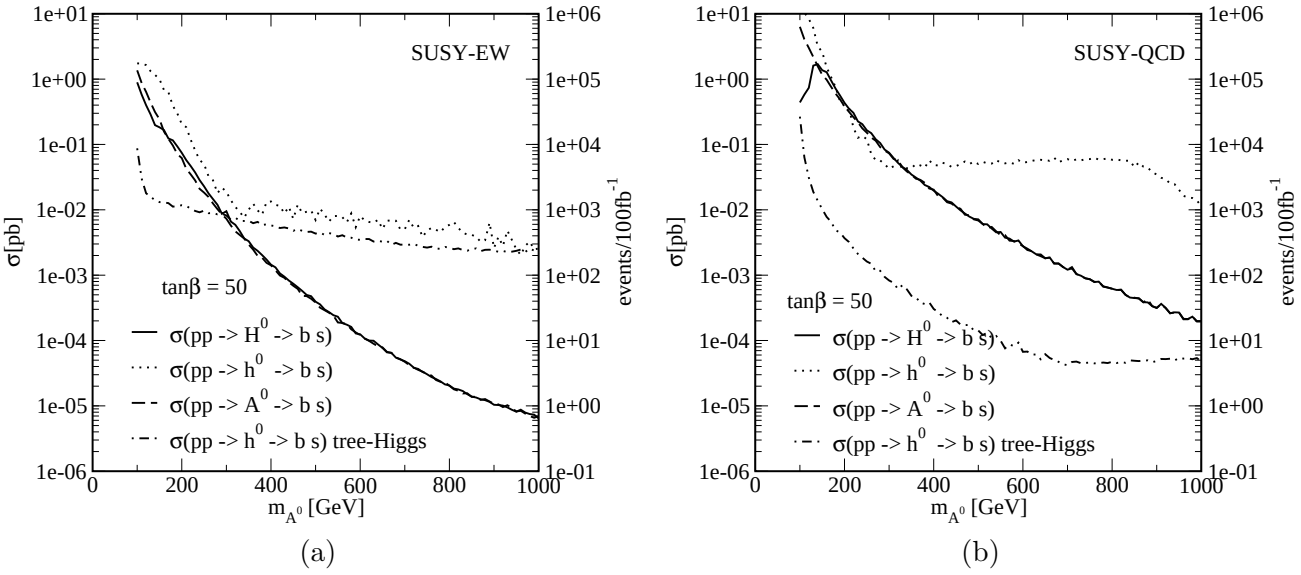

Figure 2: Maximum contributions to $\sigma(\mathrm{pp} \to h \to bs)$ in Eq. (1) as a function of m_{A^0} (at fixed $\tan\beta$) taking into account: **a**) SUSY-EW interactions with minimal flavor-mixing; **b**) SUSY-QCD interactions (see Ref. [23]). The left-vertical axis provides the cross-section (in pb) and the right-vertical axis tracks the number of events per 100 fb^{-1} of integrated luminosity.

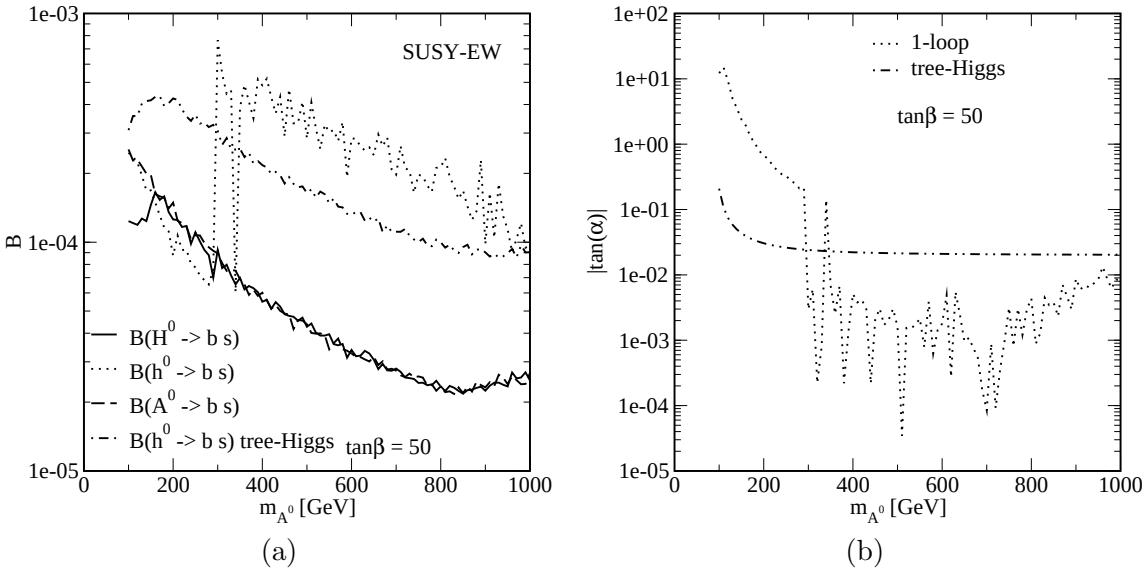

Figure 3: a) SUSY-EW contributions to the FCNC decay branching ratio $B(h \to bs)$ as a function of m_{A^0} for the MSSM parameters that maximize the various $\sigma(\mathrm{pp} \to h \to bs)$ (cf. Fig. 2a); **b)** Absolute value of $\tan\alpha$ for the parameters that maximize the specific channel $\sigma(\mathrm{pp} \to \mathrm{h}^0 \to bs)$ where the "small α_{eff} scenario" can be realized.

	H^0	h^0	A^0
$\sigma(\mathrm{pp} \to h \to bs)$	0.075 pb	0.20 pb	0.062 pb
events/100fb^{-1}	7.5×10^3	2.0×10^4	6.2×10^3
$B(h \to bs)$	1.26×10^{-4}	8.7×10^{-5}	1.5×10^{-4}
$\Gamma(h \to X)$	9.5 GeV	1.7 GeV	11.3 GeV
$\tan\alpha$	-0.30	0.67	-0.01
$m_{\widetilde{q}}$	880 GeV	660 GeV	990 GeV
μ	1000 GeV	970 GeV	1000 GeV
A_b	-2350 GeV	1900 GeV	100 GeV
A_t	-1550 GeV	-950 GeV	2000 GeV
$B(\mathrm{b} \to \mathrm{s}\gamma)$	2.1×10^{-4}	2.1×10^{-4}	2.1×10^{-4}

Table 1: Maximum MSSM value of $\sigma(\mathrm{pp} \to h \to bs)$ (and of the number of bs events per 100 fb^{-1}) at the LHC, for $m_{A^0} = 200$ GeV and $\tan\beta = 50$ under the assumption that the SUSY-QCD effects are negligible. Shown are also the corresponding values of the relevant branching ratio $B(h \to bs)$ and of the total width of the Higgs bosons ($h \equiv \mathrm{h}^0, \mathrm{H}^0, \mathrm{A}^0$), together with the values of the SUSY parameters. The last row includes $B(\mathrm{b} \to \mathrm{s}\gamma)$, which is seen to lie in the allowed experimental range.

that maximize the various $\sigma(\mathrm{pp} \to h \to bs)$. In Fig. 3b, we focus on an important feature of the particular h^0 channel, the so-called "small α_{eff} scenario" [30]. We plot there the (one-loop corrected) value of $|\tan\alpha|$ for the parameters that maximize the cross-section $\sigma(\mathrm{pp} \to \mathrm{h}^0 \to bs)$ [5]. The significant decrease of $|\tan\alpha|$ for $m_{A^0} \gtrsim 300\,GeV$ explains the relative stabilization of this cross-section in that region (cf. Fig. 2a). We have also included the corresponding curve in which the angle α is computed at the tree-level (labelled *tree-Higgs*).

In Table 1 we summarize the numerical values of $\sigma(\mathrm{pp} \to h \to bs)$, together with the parameters that maximize the production rate for $\tan\beta = 50$ at the particular point $m_{A^0} = 200$ GeV. We also provide the value of $B(h \to bs)$ and $\Gamma(h \to X)$ at the maximum of the FCNC cross-section, and the corresponding value of $B(\mathrm{b} \to \mathrm{s}\gamma)$.

Clearly, while the H^0 and A^0 channels follow a simple monotonous behavior, the particular h^0 one behaves in a complex way. Let us further elaborate on this point. At low values of $m_{A^0} \lesssim 300$ GeV, $|\tan\alpha|$ is large and in this region the radiative corrections can make it even larger (Fig. 3b). In this situation, the coupling $\mathrm{h}^0\mathrm{b}\bar{\mathrm{b}} \sim \sin\alpha/\cos\beta$ can be enhanced and the dominant production subprocess is $\sigma(pp \to \mathrm{h}^0\mathrm{b}\bar{\mathrm{b}})$. Note that, in this scenario, $\Gamma(\mathrm{h}^0 \to \mathrm{b}\bar{\mathrm{b}})$ is also enhanced whereas $B(\mathrm{h}^0 \to bs)$ is suppressed (cf. Fig. 3a). The net outcome is that the increase of the cross-section overcomes the suppression of the branching ratio and the final result is one order of magnitude larger than the *tree-Higgs* expectation – see Fig. 2a. At large values of $m_{A^0} \gtrsim 300$ GeV, instead, where the renormalized value of α (i.e. the effective α_{eff}) is significantly smaller than the tree-level prediction [30](cf. Fig. 3b), the efficiency of the production subprocess $pp \to \mathrm{h}^0\mathrm{b}\bar{\mathrm{b}}$ is severely hampered. The Higgs boson production is then dominated by gluon fusion at one loop ($gg \to \mathrm{h}^0$) and since this mechanism is controlled by the top-quark coupling $\mathrm{h}^0\mathrm{t}\bar{\mathrm{t}} \sim \cos\alpha/\sin\beta$, it becomes insensitive to variations in small α_{eff}. Adding this to the fact that $\Gamma(\mathrm{h}^0 \to \mathrm{b}\bar{\mathrm{b}})$ is strongly suppressed and $B(\mathrm{h}^0 \to bs)$ is correspondingly enhanced (cf. Fig. 3a), we end up with a regime in which the cross-section for $\mathrm{h}^0 \to bs$ production is the most favored one over a fairly sustained range of m_{A^0}.

[5] The values of $|\tan\alpha|$ shown in Fig. 3b correspond to the maximization of the SUSY-EW contributions in Fig. 2a. The corresponding values obtained from the maximization of the SUSY-QCD contributions (Fig. 2b) are essentially the same, except for the random fluctuations appearing in a Monte-Carlo computation.

The same effect was observed for the SUSY-QCD contributions [23], where the production rate is augmented some three orders of magnitude with respect to the *tree-Higgs* case (cf. Fig. 2b). The reason for this is that the SUSY-QCD effect on $\Gamma(\mathrm{h}^0 \to bs)$ is proportional to $\cos^2(\alpha-\beta)$ (see e.g. Eq. (3.5) from Ref. [22]). In the *tree-Higgs* case, this factor goes rapidly to zero for large m_{A^0} because $\alpha \to \beta - \pi/2$. However, at one loop such factor becomes $\cos^2(\alpha_{eff}-\beta)$ and the previous relation does no longer hold, so there is no such suppression. Another interesting feature to note is that the SUSY-EW contribution to $\Gamma(\mathrm{h}^0 \to bs)$ is roughly one order of magnitude smaller than the SUSY-QCD one. This property is reflected at the level of $\sigma(\mathrm{pp} \to \mathrm{h}^0 \to bs)$ (Figs. 2a,b) because in this regime the leading Higgs boson production mechanism is the same (gluon fusion) in both cases. Using our analytical approximations, we can provide a simple explanation for this numerical difference. If, for the sake of this estimate, we take all SUSY masses of the same order, the ratio between the SUSY-QCD and the SUSY-EW contributions to $\Gamma(\mathrm{h}^0 \to bs)$ is expected to be

$$\sim 10^2 \left(\frac{\alpha_s}{\alpha_W}\frac{\delta_{23}}{|V_{ts}|}\right)^2 \left(\frac{m_W}{m_t}\right)^4 \frac{1}{\tan^2\beta}\,\frac{\cos^2(\alpha_{eff}-\beta)}{\sin^2\alpha_{eff}}\,. \tag{8}$$

Here we have used the effective SUSY-QCD-induced $h^0\,b\,s$-coupling from Eq. (3.5) of Ref. [22] and the SUSY-EW contribution from the WF chargino loop effects, the latter being similar to Eq. (2) with $\cos\alpha_{eff}$ replaced by $\sin\alpha_{eff}$. The prefactor $\sim 10^2$ comes from the numerical factors $(2/3)^2\,16^2$ appearing in these formulae. For $\tan\beta = 50$ and the numerically determined values of $\delta_{23} \sim 10^{-1.5} \simeq 0.03$ and $\alpha \sim 10^{-3}$ (corresponding to large $m_{A^0} > 300\,\mathrm{GeV}$), we find that (8) is indeed of order 10, as confirmed by comparison of plots (a) and (b) in Fig. 2. This explains nicely the approximate numerical relation between the SUSY-QCD and SUSY-EW effects in the "small $\alpha_{\rm eff}$ scenario" from simple dynamical considerations. Finally, let us mention that, for very large values of m_{A^0} (namely $m_{A^0} \gtrsim 800\,\mathrm{GeV}$) the small α_{eff} scenario is no longer maintained, and so the tree-level and 1-loop values for α tend to merge (see Fig. 3). By the same token, also the two $\sigma(\mathrm{pp} \to \mathrm{h}^0 \to bs)$ curves, those for α being computed at the tree-level and at 1-loop respectively (cf. Fig. 2), tend to approach each other in the aforementioned limit[6]. It is worth recalling that the light Higgs mass (m_{h^0}) reaches its upper bound ($m_{\mathrm{h}^0} \lesssim 130\,GeV$) for $m_{A^0} \to \infty$. Since α also reaches a constant value for very large m_{A^0}, we can understand the reason why $\sigma(\mathrm{pp} \to \mathrm{h}^0 \to bs)$ exhibits an almost flat slope in this asymptotic regime.

Let us now evaluate the bs event rate attained from the direct production mechanism $\sigma(\mathrm{pp} \to bs)$. In the MSSM case, we may have both SUSY-EW and SUSY-QCD effects. The number of diagrams is rather large and, as mentioned above, it can be inferred from those in Ref. [20] after appropriate replacements of the internal and external lines. Let us first concentrate upon the purely SUSY-EW part. In Table 2 we present, in a nutshell, the predicted values for the direct production of bs pairs through gluon-gluon fusion $\sigma(\mathrm{pp(gg)} \to bs)$ from the electroweak charged-current effects (chargino and charged Higgs boson loops). The computation of $\sigma(\mathrm{pp(gg)} \to bs)$ is performed within the parameter set that optimizes the bs production rate through $\mathrm{pp} \to \mathrm{h}^0 \to bs$ (central column of Table 1). We notice that the non-standard contributions are tiny (of order 10^{-5} at most) and, moreover, a destructive interference arises when we add up the chargino and charged-Higgs boson mediated amplitudes. The latter are suppressed by small factors of m_W^2/m_H^2, m_W^2/M_{SUSY}^2 as compared to the SM ones. In addition, the GIM mechanism involved in the SM part is much less severe in the down-like quark sector as compared to its effect in the up-quark sector owing to the presence of the large top quark mass in the latter case.

Unfortunately, the probability to observe "direct bs events" does not improve in the presence of explicit sources of supersymmetric flavor mixing. In fact, our calculation of the SUSY-QCD effects on the direct bs production shows that the corresponding cross-section cannot compete with the

[6] A similar discussion, specifically for the SUSY-QCD case, can be found in Ref. [23].

partial contribution	$\sigma(\mathrm{pp(gg)} \to bs)(\mathrm{pb})$
Charged Higgs	9.7×10^{-6}
Chargino	1.1×10^{-5}
SUSY-EW	5.7×10^{-7}
MSSM	1.3×10^{-3}
SM	1.3×10^{-3}

Table 2: Different SUSY-EW contributions to the direct bs production for the choice of parameters that maximize $\sigma(\mathrm{pp} \to \mathrm{h}^0 \to bs)$ (central column of Table 1). In the absence of significant SUSY-QCD effects, the SM and the overall MSSM contributions are coincident.

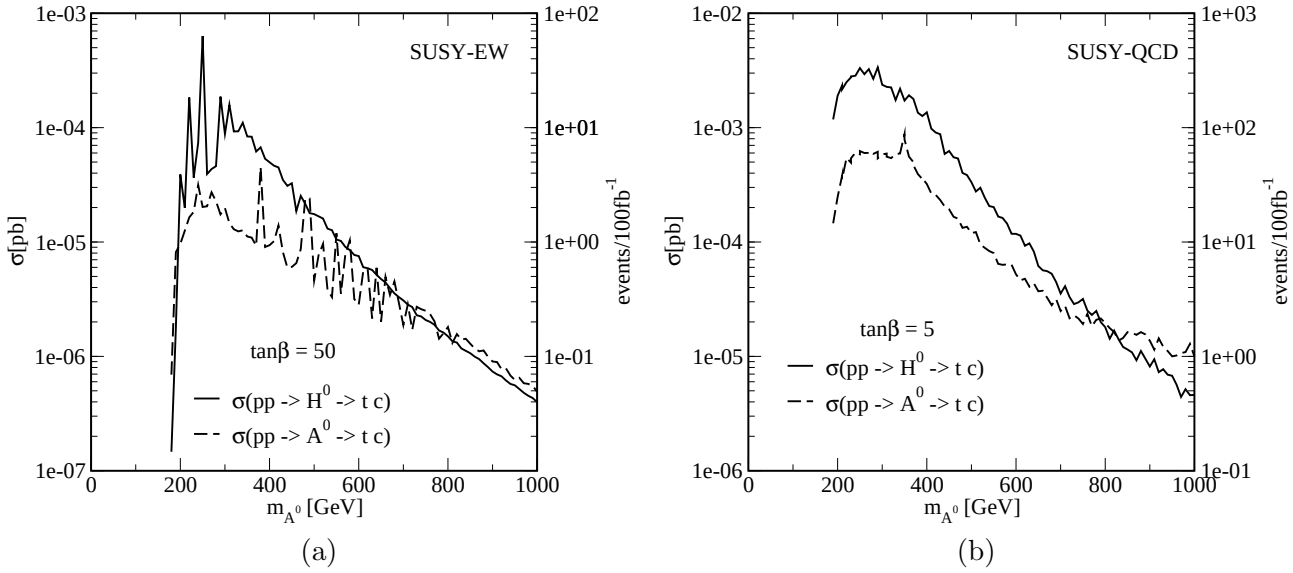

Figure 4: Maximum contributions to $\sigma(\mathrm{pp} \to h \to tc)$ – cf. Eq. (1)– as a function of m_{A^0} (at fixed $\tan\beta$) taking into account **a**) SUSY-EW interactions with minimal flavor-mixing and **b**) SUSY-QCD interactions without electroweak effects (see Ref. [23]).

FCNC Higgs boson decay channels. The reason is twofold: i) the mass insertions arising in the gluino and neutralino loops produce vertices of the guise $(\tilde{g}, \chi^0_\alpha)\, \mathrm{b}\overline{\mathrm{s}} \sim m_b(A_b - \mu \tan\beta)$ (cf. Section 2), and so proportional to m_b, whereas in the tc channel the effective vertices get a factor of m_t; ii) the particular combination $A_b - \mu \tan\beta$ becomes directly and stringently constrained by the experimental data on $B(\mathrm{b} \to \mathrm{s}\gamma)$, which impose small values of δ_{23} or very heavy gluino/neutralino masses. For example, if we take the set of MSSM parameters for which the H^0-mediated SUSY-QCD case is optimized (see Table 1 of Ref. [23]) we find $\sigma(\mathrm{pp} \to bs) = 1.1 \times 10^{-4}$ pb, versus 0.45 pb from the corresponding Higgs decay mechanism. These results can be compared with the purely SM contribution to direct bs production, which we find it to be $\sigma(\mathrm{pp} \to bs)_{\mathrm{SM}} = 1.3 \times 10^{-3}$ pb and entails ~ 100 events per $\int \mathcal{L}\, dt = 100\,\mathrm{fb}^{-1}$. We conclude that the enhancement capabilities of the bs events within the MSSM are dominated by the FCNC Higgs boson decay modes rather than by the direct FCNC production processes.

h	H^0	A^0
$\sigma(\mathrm{pp} \to h \to tc)$	8.8×10^{-5} pb	2.0×10^{-5} pb
events/100fb^{-1}	8.8	2.0
$B(h \to tc)$	8.5×10^{-7}	2.4×10^{-7}
$\Gamma(h \to X)$	36 GeV	39 GeV
$\tan\alpha$	0.046	-0.11
$m_{\widetilde{q}}$	300 GeV	350 GeV
μ	350 GeV	350 GeV
A_b	-675 GeV	-1000 GeV
A_t	20 GeV	-75 GeV
$B(\mathrm{b} \to \mathrm{s}\gamma)$	2.9×10^{-3}	2.5×10^{-3}

Table 3: Maximum SUSY-EW induced value of $\sigma(\mathrm{pp} \to h \to tc)$ (and of the number of tc events per 100 fb^{-1}) at the LHC, for $m_{A^0} = 300$ GeV and $\tan\beta = 50$. Shown are also the corresponding values of the relevant branching ratio $B(h \to bs)$ and of the total width of the Higgs bosons, together with the values of the SUSY parameters. The last row includes $B(\mathrm{b} \to \mathrm{s}\gamma)$.

5 Numerical analysis of the tc production rate

Let us now present the results of an equivalent maximization procedure for the tc production rate, $\sigma(\mathrm{pp} \to h \to tc)$. In Fig. 4a, we plot the maximum cross-sections attained at different values of the CP-odd Higgs boson mass, m_{A^0}. For better comparison, in Fig. 4b we show the corresponding maximization for the SUSY-QCD case [23]. As in the previous bs analysis, the tc production rate becomes again favored in the large $\tan\beta$ regime: this is due to the correlations between the Higgs boson production and its subsequent decay (see the analytical estimates for the tc channel in Section 2). Further numerical details of the optimal MSSM configuration are quoted in Table. 3. We find that the predicted rates are rather inconspicuous (of the order of $\sigma \sim 10^{-4}$ pb at most), and hence difficult to detect. We emphasize that this result is essentially triggered by the charginos. Neutralinos, again, have an even lesser impact. Indeed, if we recall the analytical estimates in Section 2 and the results from Tables 1 and 3, we observe that the optimal value of A_t in the latter (which is responsible for the neutralino contribution to the tc channel) is much smaller than the optimal value of A_b in the former.

It is instructive to trace the main differences between the SUSY-EW effects on the two channels (tc and bs) by using simple qualitative arguments based on the dynamical features of the MSSM. Fortunately, this can be immediately done from the analytical estimates presented in Section 2 and the optimal parameter sets in each case, which can be extracted from Tables 1 and 3. We note that the values of $\tan\alpha$ and $\tan\beta$ are quite similar in both cases. Therefore, the production cross-section obtained from the FCNC decays of the MSSM Higgs bosons must render essentially the same result and cancels in the ratio. Taking advantage of this fact, the ratio of the two cross-sections for $h = H^0, A^0$ (the two states available for both bs and tc final states) is essentially given by that of the branching ratios and also by that of the corresponding partial widths,

$$\frac{\sigma(\mathrm{pp} \to h \to bs)}{\sigma(\mathrm{pp} \to h \to tc)} \sim \frac{B(h \to bs)}{B(h \to tc)} = \frac{\Gamma(h \to bs)}{\Gamma(h \to tc)}\,. \tag{9}$$

In the specific case of the heavy CP-even neutral Higgs boson, the approximate analytical form is obtained from Eqs.(2-5). Plugging the MSSM parameters corresponding to the optimal configuration for each of the channels, we realize that the dominant contribution to bs comes from the chargino-mediated WF corrections, while the vertex corrections drive the main part of the tc one.

Therefore, we can approximate the ratio of the overall cross-sections of Eq. (9) as follows:

$$\frac{\sigma(\mathrm{pp} \to h \to bs)}{\sigma(\mathrm{pp} \to h \to tc)} \sim \left(\frac{m_t}{m_b}\right)^2 \left(\frac{A_t}{A_b}\right)^2 \sim 10^3. \tag{10}$$

which is in good agreement with the 3 orders of magnitude that arise from the exact numerical computation, once we plug the corresponding values of the quark masses and the trilinear couplings, A_t from Table 1 and A_b from Table 3. Therefore, we confirm that, in the optimal scenario, the difference between both channels can be well accounted for by the quark mass insertions squared times the ratio squared of the trilinear couplings (top quark mass and A_t, in the bs channel, versus bottom quark mass and A_b, in the tc channel).

In comparison, the situation for the direct SUSY flavor-changing production of tc pairs is remarkably distinct. As we have argued in Section 4, the enhancement factor of the relevant couplings is much larger in this case, being now proportional to the top quark mass m_t. In addition, the $\mathrm{b} \to \mathrm{s}\gamma$ constraints can be more easily eluded (just by an appropriate choice of the MSSM parameters, see Refs. [17, 20]). Numerically speaking, the direct SUSY-EW production of tc pairs furnishes $\sigma \sim 0.01\,\mathrm{pb}$, or $\sim 10^3$ events per $\int \mathcal{L}\, dt = 100$ fb^{-1} – see Ref. [20] for a comprehensive discussion including the direct SUSY-QCD effects. Such optimal scenarios are favored by relatively low supersymmetric mass scales, namely $M_{SUSY} \sim 250\,\mathrm{GeV}$, $M_1, M_2 \sim 100\,\mathrm{GeV}$ (for the electroweak soft gaugino masses), together with large flavor-mixing values of δ_{23}. The compliance with the $\mathrm{b} \to \mathrm{s}\gamma$ constraints is achieved by balancing the different SUSY-EW pieces involved in this process, i.e. assuming relatively light masses for charginos, neutralinos, charged Higgs bosons and the top squark, and also moderate values of $\tan\beta$. The dominance of the direct tc production mechanism holds also in the case of SUSY-QCD contributions [20]. In the most favorable circumstances, one can reach $\sigma \sim 1\,\mathrm{pb}$ from direct production, whereas the optimal Higgs boson-mediated output lies around $\sigma \sim 10^{-3}\,\mathrm{pb}$ (cf. Fig. 4b).

6 Discussion and conclusions

A number of studies have been devoted to the analysis of the FCNC signatures carried by electrically neutral pairs of heavy quarks of different flavors as an strategy to unravel hints of New Physics in the forthcoming LHC data. These events are very rare in the SM and, therefore, their observation could be highly revealing. Some of these studies, including ours, have focused on the possibility that the underlying new physics could be Supersymmetry, in particular the unconstrained MSSM. In this letter, we have discussed the SUSY effects on the production and subsequent FCNC decay of the neutral MSSM Higgs bosons ($h = \mathrm{h}^0, \mathrm{H}^0, \mathrm{A}^0$) into heavy quark pairs $qq' = bs, tc$ at the LHC, i.e. $\mathrm{pp} \to h \to qq'$, and we have compared the results with the direct FCNC production mechanism $\mathrm{pp} \to qq'$. Furthermore, we have computed the SUSY-EW corrections to $\sigma(\mathrm{pp} \to h \to qq')$ and also the SUSY-QCD and SUSY-EW contributions to $\sigma(\mathrm{pp} \to bs)$. These results extend the analyses previously presented for the SUSY-QCD effects on $\sigma(\mathrm{pp} \to h \to qq')$ [23] and the SUSY-QCD and SUSY-EW ones on $\sigma(\mathrm{pp} \to tc)$ [16–18, 20]. At the end of the day, we have nicely completed the map of MSSM predictions for the heavy qq'-pairs produced at the LHC.

The upshot of this lengthy investigation, which includes also the analyses from the previous works [17, 20, 22, 23]), is summarized in Table 4. These numerical results are obtained in full consistency with the stringent experimental constraints from $\mathrm{b} \to \mathrm{s}\gamma$. The most favorable channels turn out to be the following: 1) the Higgs boson FCNC decays into bs, and 2) the direct production of tc pairs, both of them with maximal cross-sections of $\sim$ 1pb and dominated by SUSY-QCD effects. In that table, we also collect the results $\sigma(\mathrm{pp} \to bs)_{\max} \sim 10^{-3}$pb from SUSY-QCD and $\sim 10^{-4}$pb from SUSY-EW. Clearly, the direct production of bs pairs in the MSSM is highly inefficient as compared to the rate that could originate from FCNC decays of the MSSM Higgs

FCNC mechanism channel	$t-c$	$b-s$
Higgs decay-mediated mechanism		
SUSY-QCD	$\sim 10^{-3}\,\text{pb}$	$\sim 1\,\text{pb}$
SUSY-EW	$\sim 10^{-4}\,\text{pb}$	$\sim 10^{-1}\,\text{pb}$
Direct FCNC production mechanism		
SUSY-QCD dominance	$\sim 1\,\text{pb}$	$\sim 10^{-3}\,\text{pb}$
SUSY-EW dominance	$\sim 10^{-2}\,\text{pb}$	$\sim 10^{-4}\,\text{pb}$
SM	$\sim 10^{-7}\,\text{pb}$	$\sim 10^{-3}\,\text{pb}$

Table 4: Summary of optimal SUSY contributions for tc and bs events at the LHC, within order of magnitude. For the direct production, we follow the same procedure as in [20], viz. we explore scenarios where there is a dominant SUSY component (SUSY-EW or SUSY-QCD) and allow a smaller contribution from the other. In the last row, we quote the SM prediction.

bosons. Finally, if the SUSY-QCD part is negligible (e.g. because the gluinos are very heavy or the flavor-mixing terms are too small), the SUSY-EW loops alone yield a small tc rate from Higgs boson decays, $\sigma(\text{pp} \to h \to tc)_{\max} \sim 10^{-4}\text{pb}$. Nonetheless, in this case, we also have $\sigma(\text{pp} \to h \to bs)_{\max} \sim 0.1\text{pb}$, implying $\sim 10^4$ bs pairs per $100\,\text{fb}^{-1}$ of integrated luminosity. In other words, in the absence of strong supersymmetric interactions, the tc signature disappears for all practical purposes but we could still count on a fairly large amount of bs events triggered by electroweak supersymmetric sources.

Despite the predicted number of FCNC $q\,q'$ events is sizeable in some cases, it is far from obvious that they could be efficiently disentangled from the underlying background of QCD jets where they would be immersed, even in the most favorable conditions. For example, it is well known that the simple two-body decay $h \to \text{b}\,\overline{\text{b}}$ is virtually impossible to isolate, due to the huge irreducible QCD background from $\text{b}\,\overline{\text{b}}$ dijets. This led, long time ago, to complement the search with many other channels, particularly with the radiative decay $h \to \gamma\,\gamma$, which has been identified as an excellent signature in the appropriate range [10]. Similarly, the FCNC Higgs boson decay channels may help to complement the general Higgs boson search strategies, mainly because the FCNC processes should be essentially free of QCD background. Notwithstanding, other difficulties can appear related to the misidentification of jets. For instance, for the bs final states misidentification of b quarks as c quarks in cs-production from charged currents may obscure the possibility that the bs events can be really attributed to Higgs boson FCNC decays. This also applies to the tc final states [39], where misidentification of b quarks as c quarks in e.g. tb-production, might be a source of background to the tc events, although in this case the clear-cut top quark signature should be much more helpful (specially after performing a study of the distribution of the signal versus the background). These studies, however, go beyond the scope of the analysis presented in this work.

To summarize, in this letter we have completed the calculations necessary to account for the FCNC-triggered qq' events that could emerge at the LHC from supersymmetric sources in the unconstrained MSSM. While admitting that the practical detection of these events can be difficult, the message from the theoretical side seems now crystal-clear: the MSSM has the potential to provide large amounts of heavy quark pairs from genuine supersymmetric FCNC interactions, to wit: in the bs channel, the production and subsequent FCNC decay of a neutral Higgs boson entails potentially large enhancements (mainly in the large $\tan\beta$ regime) which could boost the predicted cross-sections up to $\sigma(\text{pp} \to h \to bs) \sim 1\,\text{pb}$ from SUSY-QCD, and $\sim 0.1\,\text{pb}$ from SUSY-EW, whilst the direct production is not enhanced at all with respect to the SM result. At variance with

this situation, the tc channel can be maximally enhanced from the direct mechanism, whereas the Higgs boson-mediated rate $\sigma(\mathrm{pp} \to h \to tc)$ proves to be negligible. From the SUSY-QCD side, we find the direct production cross-section $\sigma(\mathrm{pp} \to tc)_{\max} \sim 1\,\mathrm{pb}$, while from SUSY-EW we obtain $\sigma_{\max}(\mathrm{pp} \to tc) \sim 0.01\,\mathrm{pb}$, the respective number of events being rather large: 10^5 and 10^3 tc pairs per $\int \mathcal{L}\,dt = 100\,\mathrm{fb}^{-1}$. The tc signature should obviously be the preferred one for a more promising experimental tagging owing to the presence of the top quark in the final state.

Acknowledgements

The work of SB has been supported by European Community's Marie-Curie Research Training Network under contract MRTN-CT-2006-035505 'Tools and Precision Calculations for Physics Discoveries at Colliders' ; DLV by the MEC FPU grant Ref. AP2006-00357; JG and JS in part by MEC and FEDER under project FPA2007-66665 and also by DURSI Generalitat de Catalunya under project 2005SGR00564. This work has also been supported by the Spanish Consolider-Ingenio 2010 program CPAN CSD2007-00042.

References

[1] H. P. Nilles, Phys. Rept. **110**, 1 (1984); H. E. Haber and G. L. Kane, Phys. Rept. **117**, 75 (1985); A. B. Lahanas and D. V. Nanopoulos, Phys. Rept. **145**, 1 (1987).

[2] J. A. Grifols and J. Solà, Phys.Lett. **B137**, 257 (1984); Nucl. Phys. **B253**, 47 (1985); D. Garcia and J. Solà, Mod. Phys. Lett. **A9**, 211 (1994); D. Garcia, R. A. Jiménez and J. Solà, Phys. Lett. **B347**, 309 (1995); Phys. Lett. **B347**, 321 (1995).

[3] P.H. Chankowski, A. Dabelstein, W. Hollik, W.M. Mosle, S. Pokorski, J. Rosiek, Nucl. Phys. B417, 101 (1994).

[4] S. L. Glashow, J. Iliopoulos and L. Maiani, Phys. Rev. **D2**, 1285 (1970).

[5] W. M. Yao et al. (Particle Data Group Collaboration), J. Phys. **G33**, 1 (2006).

[6] J. L. Diaz-Cruz, R. Martinez, M. A. Perez and A. Rosado, Phys. Rev. **D41**, 891 (1990); G. Eilam, J. L. Hewett and A. Soni, Phys. Rev. **D44**, 1473 (1991); B. Mele, S. Petrarca and A. Soddu, Phys. Lett. **B435**, 401 (1998), `hep-ph/9805498`; J. A. Aguilar-Saavedra, Acta Phys. Polon. **B35**, 2695 (2004), `hep-ph/0409342`.

[7] J. Guasch and J. Solà, Nucl. Phys. **B562**, 3 (1999), `hep-ph/9906268`.

[8] J.-M. Yang and C.-S. Li, Phys. Rev. **D49**, 3412 (1994).

[9] M. Misiak, S. Pokorski and J. Rosiek, Adv. Ser. Direct. High Energy Phys. **15**, 795–828 (1998), `hep-ph/9703442`.

[10] J. F. Gunion, H. E. Haber, G. L. Kane and S. Dawson, *The Higgs hunter's guide*, Addison-Wesley, Menlo-Park, 1990.

[11] S. Béjar, J. Guasch and J. Solà, Nucl. Phys. **B600**, 21 (2001), `hep-ph/0011091`.

[12] S. Béjar, J. Guasch and J. Solà, Nucl. Phys. **B675**, 270 (2003), `hep-ph/0307144`.

[13] A. Arhrib, Phys. Lett. **B612**, 263 (2005), `hep-ph/0409218`; A. Arhrib, Phys. Rev. **D72**, 075016 (2005), `hep-ph/0510107`; I. Baum, (2007), `arXiv:0711.1311 [hep-ph]`.

[14] G. Burdman, Phys. Rev. Lett. 83 (1999) 2888, hep-ph/9905347; J.-j. Cao, Z.-h. Xiong and J. M. Yang, Phys. Rev. **D67**, 071701 (2003), hep-ph/0212114; P. M. Ferreira, O. Oliveira and R. Santos, Phys. Rev. **D73**, 034011 (2006), hep-ph/0510087; P. M. Ferreira and R. Santos, Phys. Rev. **D73**, 054025 (2006), hep-ph/0601078; P. M. Ferreira, R. B. Guedes and R. Santos, (2008), arXiv:0802.2075 [hep-ph].

[15] S. Béjar, J. Guasch and J. Solà, (2001), hep-ph/0101294, in: Proc. of the 5th International Symposium on Radiative Corrections (RADCOR 2000), Carmel, California, 11-15 Sep 2000; S. Béjar, hep-ph/0606138.

[16] J. J. Liu, C. S. Li, L. L. Yang and L. G. Jin, Nucl. Phys. **B705**, 3 (2005), hep-ph/0404099.

[17] J. Guasch, W. Hollik, S. Peñaranda and J. Solà, Nucl. Phys. Proc. Suppl. **157**, 152 (2006), hep-ph/0601218; J. Solà, talk at RADCOR 2005, Shonan Village, Japan, October 2-7 2005, *Single top quark production by direct supersymmetric FCNC interactions at the LHC* , http://www-conf.kek.jp/radcor05/.

[18] G. Eilam, M. Frank and I. Turan, Phys. Rev. **D74**, 035012 (2006), hep-ph/0601253.

[19] J. Cao, G. Eilam, K.-i. Hikasa and J. M. Yang, Phys. Rev. **D74**, 031701 (2006), hep-ph/0604163; J. J. Cao et al., Phys. Rev. **D75**, 075021 (2007), hep-ph/0702264; J. L. Diaz-Cruz, H.-J. He and C. P. Yuan, Phys. Lett. **B530**, 179 (2002), hep-ph/0103178.

[20] D. López-Val, J. Guasch and J. Solà, JHEP **12**, 054 (2007), arXiv:0710.0587 [hep-ph]; arXiv:0801.2469 [hep-ph].

[21] A. M. Curiel, M. J. Herrero and D. Temes, Phys. Rev. **D67**, 075008 (2003), hep-ph/0210335.

[22] S. Béjar, F. Dilmé, J. Guasch and J. Solà, JHEP **08**, 018 (2004), hep-ph/0402188

[23] S. Béjar, J. Guasch and J. Solà, JHEP **10**, 113 (2005), hep-ph/0508043; Nucl. Phys. Proc. Suppl. **157**, 147 (2006), hep-ph/0601191.

[24] D. A. Demir, Phys. Lett. **B571**, 193 (2003), hep-ph/0303249.

[25] A. M. Curiel, M. J. Herrero, W. Hollik, F. Merz and S. Peñaranda, Phys. Rev. **D69**, 075009 (2004), hep-ph/0312135.

[26] T. Hahn, W. Hollik, J. I. Illana and S. Peñaranda, (2005), hep-ph/0512315.

[27] A. Arhrib, D. K. Ghosh, O. C. W. Kong and R. D. Vaidya, Phys. Lett. **B647**, 36–42 (2007), hep-ph/0605056.

[28] For an overview, see D. López-Val, talk at: Interplay of collider and flavor physics workshop, CERN, Geneve, December 2-3 2007, http://indico.cern.ch/conferenceDisplay.py?confId=22180.

[29] J. A. Coarasa, D. Garcia, J. Guasch, R. A. Jiménez and J. Solà, Eur. Phys. J. **C2**, 373 (1998), hep-ph/9607485; R. A. Jiménez and J. Solà, Phys. Lett. **B389** 53 (1996), hep-ph/9511292; J.A. Coarasa, R. A. Jimenez, J. Solà, Phys. Lett. **B389** 312 (1996), hep-ph/9511402.

[30] M. Carena, S. Mrenna and C. E. M. Wagner, Phys. Rev. **D62**, 055008 (2000), hep-ph/9907422; M. Carena, S. Heinemeyer, C. E. M. Wagner and G. Weiglein, Eur. Phys. J. **C26**, 601 (2003), hep-ph/0202167.

[31] M. Spira, HIGLU and HQQ packages: http://people.web.psi.ch/∼spira/higlu/, and http://people.web.psi.ch/∼spira/hqq/; M. Spira, (1995), hep-ph/9510347; M. Spira, A. Djouadi, D. Graudenz and P. M. Zerwas, Nucl. Phys. **B453**, 17 (1995), hep-ph/9504378; M. Spira, Fortsch. Phys. **46**, 203 (1998), hep-ph/9705337, and references therein.

[32] T. Hahn and M. Pérez-Victoria, Comput. Phys. Commun. **118**, 153 (1999), hep-ph/9807565; T. Hahn, *LoopTools* user's guide, available from http://www.feynarts.de/looptools; G. J. van Oldenborgh and J. A. M. Vermaseren, Z. Phys. **C46**, 425 (1990); T. Hahn, *FeynArts 2.2*, *FormCalc* and *LoopTools* user's guides, available from http://www.feynarts.de.

[33] O. Brein, Comput. Phys. Commun. **170**, 42 (2005), hep-ph/0407340.

[34] G. P. Lepage, J. Comput. Phys. **27**, 192 (1978).

[35] D. Stockinger, J. Phys. **G34**, R45 (2007), hep-ph/0609168.

[36] C. Bobeth, M. Misiak and J. Urban, Nucl. Phys. **B567**, 153 (2000), hep-ph/9904413.

[37] P. Gambino, U. Haisch and M. Misiak, Phys. Rev. Lett. **94**, 061803 (2005), hep-ph/0410155.

[38] A. Denner, Fortschr. Phys. **41**, 307 (1993), arXiv:0709.1075 [hep-ph].

[39] T. Stelzer, Z. Sullivan and S. Willenbrock, Phys. Rev. **D58**, 094021 (1998), hep-ph/9807340; Z. Sullivan, Phys. Rev. **D70**, 114012 (2004), hep-ph/0408049.